Published August 2, 2010

γ-Tubulin regulates the anaphase-promoting complex/cyclosome during interphase

Tania Nayak,[1] Heather Edgerton-Morgan,[1,2] Tetsuya Horio,[2] Yi Xiong,[1] Colin P. De Souza,[1] Stephen A. Osmani,[1] and Berl R. Oakley[1,2]

[1]Department of Molecular Genetics, The Ohio State University, Columbus, OH 43210
[2]Department of Molecular Biosciences, The University of Kansas, Lawrence, KS 66045

A cold-sensitive γ-tubulin allele of *Aspergillus nidulans*, *mip*AD159, causes defects in mitotic and cell cycle regulation at restrictive temperatures that are apparently independent of microtubule nucleation defects. Time-lapse microscopy of fluorescently tagged mitotic regulatory proteins reveals that cyclin B, cyclin-dependent kinase 1, and the Ancdc14 phosphatase fail to accumulate in a subset of nuclei at restrictive temperatures. These nuclei are permanently removed from the cell cycle, whereas other nuclei, in the same multinucleate cell, cycle normally, accumulating and degrading these proteins. After each mitosis, additional daughter nuclei fail to accumulate these proteins, resulting in an increase in noncycling nuclei over time and consequent inhibition of growth. Extensive analyses reveal that these noncycling nuclei result from a nuclear autonomous, microtubule-independent failure of inactivation of the anaphase-promoting complex/cyclosome. Thus, γ-tubulin functions to regulate this key mitotic and cell cycle regulatory complex.

Introduction

γ-Tubulin is a component of microtubule-organizing centers and is conserved in all eukaryotes. Its role as a nucleator of spindle and cytoplasmic microtubules is well established (for reviews see Wiese and Zheng, 1999; Oakley, 2000; Job et al., 2003), but evidence has emerged from several sources that γ-tubulin and γ-tubulin ring complex proteins have microtubule-independent roles in mitotic regulation (for reviews see Lange, 2002; Cuschieri et al., 2007). Our laboratory has generated a collection of mutant alleles of *mipA*, the *Aspergillus nidulans* γ-tubulin gene (Jung et al., 2001). One cold-sensitive allele, *mip*AD159, disrupts the coordination of late mitotic events such as chromosomal disjunction and mitotic exit at restrictive temperatures (Prigozhina et al., 2004). We reasoned that examining the localization of mitotic regulatory proteins in strains carrying *mip*AD159 would likely reveal the nature of mitotic misregulation caused by this allele and, thus, clarify the functions of γ-tubulin in mitotic regulation.

Using recent advances in gene targeting techniques in *A. nidulans* (Yang et al., 2004; Nayak et al., 2006; Szewczyk et al., 2006), we fused GFP, monomeric RFP (mRFP), or mCherry to the C terminus of several mitotic regulatory proteins and studied their localization in strains carrying the wild-type *mipA* allele (*mipA*+) and strains carrying *mip*AD159. Although the localization of some proteins was not altered in an informative way, three proteins, cyclin B, Cdk1, and Ancdc14, showed a dramatic alteration of localization. *A. nidulans* is coenocytic, and nuclei within a cell go through the cell cycle synchronously, with mitotic regulatory proteins such as cyclin B accumulating and being destroyed at the same time in all nuclei. In strains carrying *mip*AD159, at restrictive temperatures, cyclin B, Cdk1, and Ancdc14 failed to accumulate in a subset of the nuclei within a cell. Time-lapse imaging revealed that these nuclei were removed from the cell cycle and that the fraction of noncycling nuclei increased with each cell cycle. Extensive experimental analyses indicate that these noncycling nuclei result from

Correspondence to Berl R. Oakley: boakley@ku.edu

T. Nayak's present address is Dept. of Pathology and Cell Biology, Columbia University College of Physicians and Surgeons, New York, NY 10032.

Abbreviations used in this paper: APC/C, anaphase-promoting complex/cyclosome; CB−, cyclin B negative; CB+, cyclin B positive; dbΔ–cyclin B–GFP, destruction box–deleted cyclin B–GFP; mRFP, monomeric RFP; NLS-DsRed, nuclear localization signal fused to DsRed fluorescent protein; NPC, nuclear pore complex; SAC, spindle assembly checkpoint; SPB, spindle pole body.

Supplemental Material can be found at:
http://jcb.rupress.org/content/suppl/2010/07/29/jcb.201002105.DC1.html

The Rockefeller University Press $30.00
J. Cell Biol. Vol. 190 No. 3 317–330
www.jcb.org/cgi/doi/10.1083/jcb.201002105

Published August 2, 2010

*mipA*D159 causing a nuclear autonomous failure of inactivation of the anaphase-promoting complex/cyclosome (APC/C) in the G_1 phase of the cell cycle.

Results

Creation of fluorescent fusion proteins

Unless otherwise mentioned, all imaging was performed with proteins tagged at their C termini by using fusion PCR to create transforming DNA fragments in which the 3′ end of the target gene was fused in frame to a GFP, mCherry, or mRFP coding sequence. The fusion genes were the only copies in the genome. They were under the control of their endogenous promoters, and the fusion proteins appeared to be fully functional, supporting normal growth over a wide range of temperatures (from 20 to 42°C) and causing no apparent mitotic or cell cycle defects. Genotypes of strains are shown in Table S1.

In vivo localization of cyclin B and Cdk1 through the cell cycle

In *A. nidulans*, only hyphal tip cells are mitotically active, and all observations and experiments involving the cell cycle were performed with tip cells. The localization patterns of cyclin B and Cdk1 were very similar (as expected because Cdk1 is localized to the nucleus through its binding to cyclin B; Nurse, 1990), and we will discuss them together. Cyclin B is the only essential cyclin in *A. nidulans*, and it is encoded by the *nimE* gene (Morris, 1975; O'Connell et al., 1992; Osmani et al., 1994). In *A. nidulans*, there is a single Cdk1 gene, *nimX*, and it is required for progression through G_1 and G_2 (Osmani et al., 1994).

We performed time-lapse imaging of strains LO1438 and LO3317, expressing cyclin B–GFP and histone H1–mRFP to allow visualization of chromatin (Nayak et al., 2006). The timing of cell cycle stages in *A. nidulans* has been determined with precision (Bergen and Morris, 1983), and chromosomes visibly condense in mitosis, so it is possible to correlate our observations with cell cycle stages with reasonable confidence. Cyclin B–GFP was not visible in early G_1 nuclei but became visible as nuclei progressed through interphase (Fig. 1 A). In 346 randomly selected interphase tip cells, 61.0% of cells (weighted mean of four experiments; weighted SD = 3.4%) had visible cyclin B–GFP in their nuclei. Thus, cyclin B becomes visible ∼40% of the way through interphase, and this point corresponds to S phase (Bergen and Morris, 1983). Because cyclin B must accumulate to some extent before we can detect it, the point at which cyclin B begins to accumulate in nuclei is earlier, logically at the G_1/S boundary because cyclin B and Cdk1 are required for DNA synthesis in *A. nidulans* (Osmani et al., 1994). Cyclin B–GFP fluorescence was visible in the nucleoplasm and, more intensely, at spindle pole bodies (SPBs). The signal increased as the cell cycle proceeded (Fig. 1 A), which is consistent with previous observations (Wu et al., 1998; De Souza et al., 2009).

The localization pattern of cyclin B in mitosis in living cells has been described recently (De Souza et al., 2009), and our observations are largely consistent with these data. At mitotic entry, when the nuclear pore complex (NPC) partially disassembles (De Souza et al., 2004), much of the cyclin B rapidly exited the nuclei, but a fraction remained in the nucleoplasm and at the SPB (Fig. 1 B). As mitosis proceeded (Fig. 1 B), SPBs separated, and cyclin B–GFP was concentrated at the SPBs and between the SPBs (i.e., on the spindle) but was visible at a lower intensity throughout the nucleus. The concentration of cyclin B at the SPB and on the mitotic spindle was reduced to the levels in the general nucleoplasm by 30–90 s before anaphase onset (data from 21 nuclei observed by dual-wavelength time-lapse imaging with z-series stacks [0.4-µm step size] collected at 30-s intervals at 25 ± 1°C). The remaining cyclin B disappeared gradually. In 9/21 cases, it was undetectable by the end of anaphase A, in 9/21 cases, it persisted into anaphase B/telophase, and in 3/21 cases, it was present in anaphase A but gone by the earliest anaphase B time point 30 s later.

A. nidulans cells are multinucleate, and the nuclei within a cell go through the cell cycle in synchrony. Nuclei at one end of the cell enter mitosis first, and a wave of mitosis sweeps rapidly through the cell. Cyclin B–GFP fluorescence was essentially identical in all nuclei within a tip cell in interphase, and nuclei showed the same pattern of cyclin B–GFP destruction as the mitotic wave progressed through the cell.

In *A. nidulans*, multiple rounds of mitosis occur before the first cell division (septation) occurs. After each subsequent mitosis, septation occurs asymmetrically, dividing the hypha into a mitotically active tip cell and mitotically inactive subapical cells. We found that cyclin B does not accumulate in the nuclei in subapical cells (Fig. 1 A), indicating that they are blocked in G_1. Cyclin B did accumulate again in subapical cells when a side branch with a growing tip formed, restarting the cell cycle.

The Cdk1-GFP localization pattern was very similar to that of cyclin B. Simultaneous time-lapse imaging of cyclin B–GFP and Cdk1-mCherry (strain LO1851) revealed that the two proteins appeared in the nucleus at the same time, increased in brightness as the cell cycle progressed, and disappeared from nuclei during mitosis. A surprising difference, however, was that Cdk1 consistently exited from mitotic nuclei ∼1.5 min before cyclin B–GFP had completely disappeared (Fig. 2). This suggests that a portion of Cdk1 is released before cyclin B is destroyed. Release of Cdk1 from cyclin B has been studied surprisingly little, perhaps because the assumption has been that the destruction of cyclin B by the proteasome causes release of Cdk1. However, the available evidence (Nishiyama et al., 2000; Chesnel et al., 2006) from in vitro studies suggests that the proteasome actually causes release of Cdk1 by a mechanism that precedes and is independent of proteolysis. Our observations provide in vivo results supporting these data.

Cyclin B, Cdk1, and Ancdc14 fail to accumulate in a subset of nuclei in a γ-tubulin mutant strain

To determine whether cyclin B localization was altered by *mipA*D159, we observed a strain (LO1439) carrying cyclin B–GFP, histone H1–mRFP, and *mipA*D159 at a restrictive temperature of 25°C. Many nuclei divide normally at 25°C in strains carrying *mipA*D159, whereas others exhibit chromosomal segregation abnormalities (Prigozhina et al., 2004). We found that cyclin B localization patterns in mitosis were

Published August 2, 2010

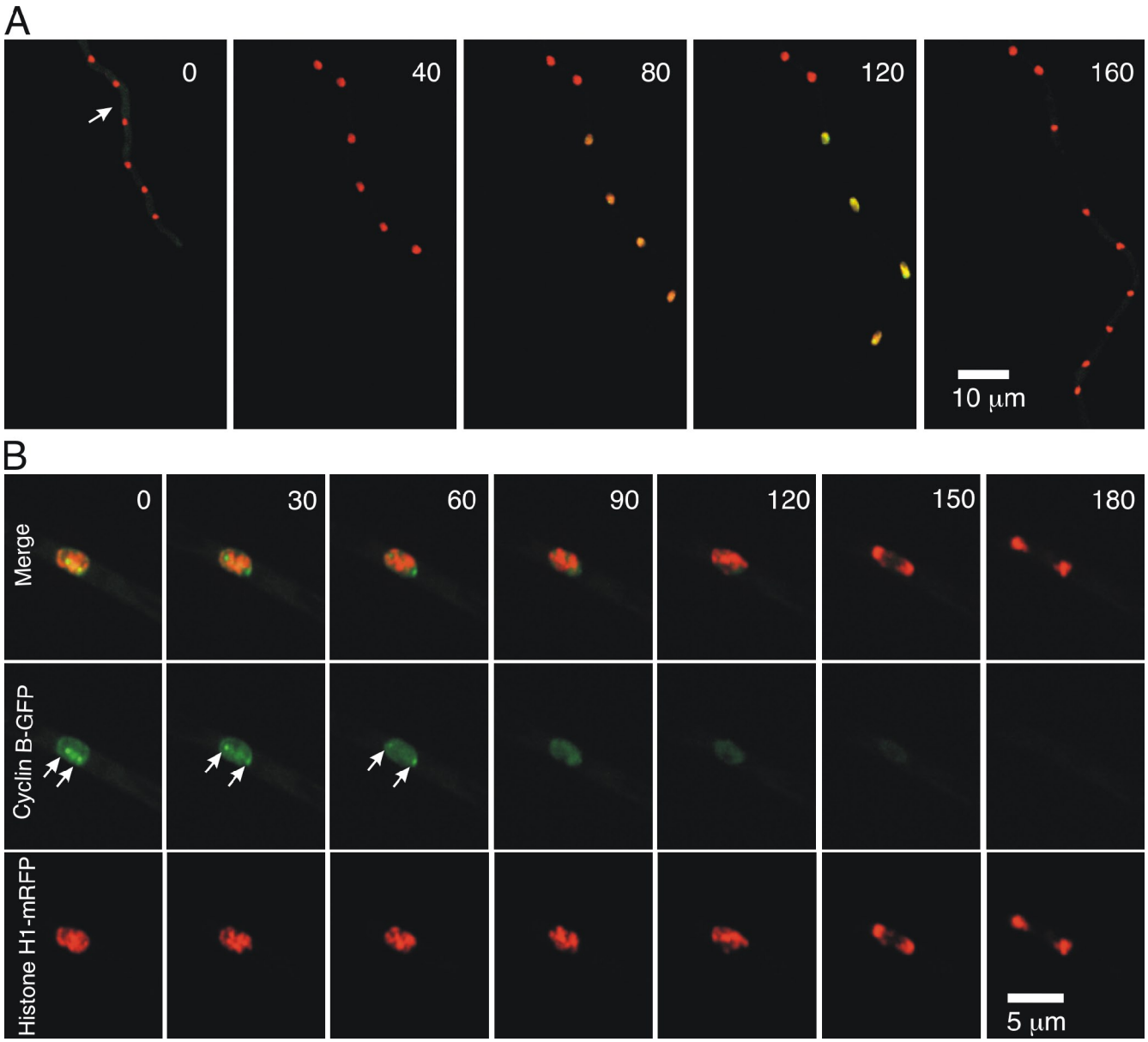

Figure 1. **Accumulation and destruction of cyclin B through the cell cycle.** (A) Images are projections of z-series stacks of cyclin B–GFP and histone H1–mRFP from a time-lapse dataset captured at 25°C with a spinning-disk confocal microscope (strain LO3317). At t = 0, nuclei have just completed mitosis. A septum formed afterward (position shown by arrow) such that the top two nuclei are in a separate subapical cell, and they do not cycle or accumulate cyclin B. The bottom four nuclei are in the same apical cell and accumulate cyclin B synchronously (nuclei becoming yellow at 80- and 120-min time points). They go through mitosis between the 140- (not depicted) and 160-min time points, and cyclin B is destroyed. (B) Destruction of cyclin B during mitosis in wild-type *A. nidulans*. The images are projections of z-series stacks captured at 30-s intervals at 25°C with a spinning-disk confocal system. At t = 0 (which is prophase based on SPB separation and positioning of condensed chromosomes), cyclin B is localized throughout the nucleoplasm but is most prominent at SPBs (arrows) and in the region between the SPBs. As the mitotic spindle (not depicted) elongates, the SPBs move farther apart (30 s). Destruction of cyclin B occurs first at SPBs and the spindle region (60- and 90-s time points) and is destroyed in the remainder of the nucleoplasm. Most cyclin B has been destroyed by late anaphase (150 s) in this nucleus, although cyclin B was visible at telophase in some nuclei.

normal in many nuclei, but we noted two alterations in nuclei undergoing abnormal mitosis. First, cyclin B remained at the poles for an extended period in some such nuclei, and chromatin did not decondense until cyclin B had disappeared. This presumably reflects the fact that cyclin B is involved in the monitoring of the successful completion of mitosis and that destruction of cyclin B is important for mitotic exit (Murray et al., 1989; Nurse, 1990; for review see Pines and Rieder, 2001). Second, cyclin B was often localized into clumps (Fig. S1 A), a localization pattern that was never seen in *mipA*+ controls. The cyclin B in these clumps disappeared over time, coincident with chromatin decondensation, but mitosis was usually not completed successfully.

However, the most striking defect was that a subset of nuclei failed to accumulate cyclin B in interphase, whereas other nuclei in the same cell accumulated it normally and passed through the cell cycle successfully (Fig. 3). The presence of such cyclin B–negative (CB−) nuclei was quite surprising in that, as mentioned, nuclei within a single-tip cell normally pass through the cell cycle in synchrony and behave identically with respect to the accumulation of cyclin B.

Published August 2, 2010

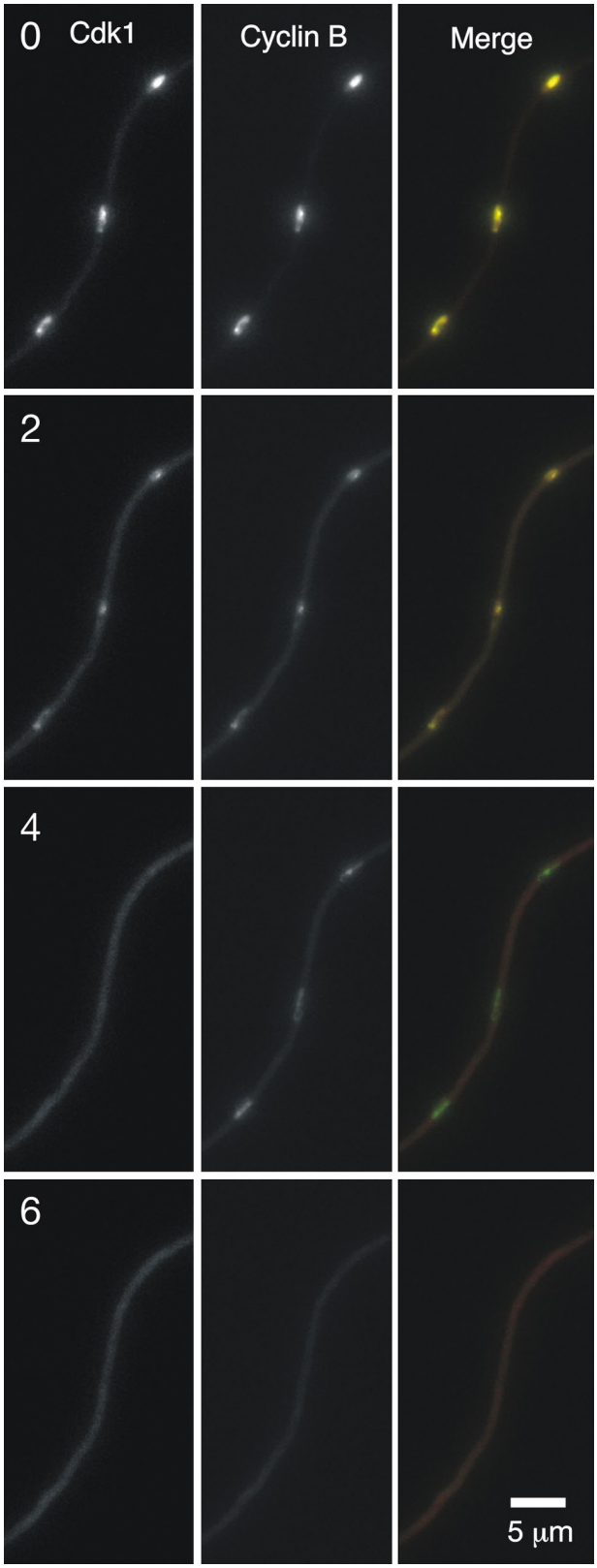

Figure 2. **Cdk1 leaves the nucleoplasm before cyclin B is completely destroyed.** Cdk1-mCherry is shown in red, and cyclin B–GFP is shown in green in the merge panel. The time of capture (in minutes) is shown at the top left of each row. At t = 0, immediately before mitosis, Cdk1 and cyclin B localization is nearly identical. At 2 min, some Cdk1 and cyclin B moves from the nucleus to the cytoplasm as indicated by weaker nuclear fluorescence and brighter cytoplasmic fluorescence. From observations of strains carrying cyclin B–GFP and other tagged proteins such as histone H1 mRFP, we know that the cyclin B exit occurs at the G_2 to M transition. At 4 min, Cdk1 has exited the nucleus but cyclin B fluorescence remains, and at 6 min, cyclin B has gone.

Cdk1-GFP had a similar localization pattern to cyclin B in a strain carrying *mipA*D159 (LO4031) at the same restrictive temperature and was completely absent from some nuclei in cells in which most nuclei had accumulated Cdk1 (Fig. S1 B). We imaged a strain carrying *mipA*D159, cyclin B–GFP, and Cdk1-mCherry (LO2586) at the restrictive temperature and found that no cyclin B–positive (CB+) nuclei were Cdk1 negative and vice versa. Thus, we infer that all Cdk1-negative nuclei are also CB−.

The homologue of *Saccharomyces cerevisiae* cdc14p exhibited a similar accumulation defect. This protein plays a critical role in mitotic regulation in some organisms (Jaspersen et al., 1998; Visintin et al., 1998; for review see Stegmeier and Amon, 2004). The *A. nidulans* cdc14 homologue has been identified (Son and Osmani, 2009) and designated An*cdc14*. It is not essential for mitosis (Son and Osmani, 2009).

Time-lapse observations of a strain (LO1517) carrying An*cdc14*-GFP and histone H1–mRFP revealed that Ancdc14 (the product of the An*cdc14* gene) begins to be visible in S phase, slightly after Cdk1 is detectable. Interestingly, Ancdc14-GFP does not localize to the nucleolus in *A. nidulans* (Fig. 4) as its homologues do in *S. cerevisiae* and *Schizosaccharomyces pombe* (for review see Stegmeier and Amon, 2004). It increases in intensity within nuclei as they pass through interphase, displays a complex localization in mitosis, and localizes to the forming septum after mitosis is completed. Time-lapse imaging of a strain carrying *mipA*D159, Ancdc14-GFP, and histone H1–mRFP (LO1532) revealed that, at a restrictive temperature, Ancdc14-GFP accumulated normally at septa but, like cyclin B and Cdk1, failed to accumulate in a subset of nuclei (Fig. 4).

To determine whether the nuclei that fail to accumulate Ancdc14 are the same as those that lack Cdk1 and, by inference, cyclin B, we imaged Ancdc14-GFP and Cdk1-mCherry in a strain carrying *mipA*D159 (LO4322). Because Cdk1 is detectable earlier in the cell cycle than Ancdc14, we only scored nuclei in cells in which Ancdc14-GFP was present in some nuclei. Of 139 Ancdc14-GFP–positive nuclei scored, only two (1.4%) were Cdk1-mCherry negative. Nearly all nuclei that accumulate Ancdc14 also accumulate Cdk1, and we can infer that nearly all Ancdc14-negative nuclei also fail to accumulate Cdk1 and cyclin B.

Analysis of the failure of cyclin B accumulation by time-lapse imaging

To investigate the failure of cyclin B/Cdk1 and Ancdc14 accumulation, we focused our attention on cyclin B because it is essential for cell cycle progression and because Cdk1 localization depends on cyclin B (for review see Nigg, 1995). We imaged strain LO1439 (cyclin B–GFP, histone H1–mRFP, and *mipA*D159) incubated at a restrictive temperature of 25°C from the time of germination (11 h after inoculation) through as many as five rounds of mitosis (20 h of imaging per sample). We first

Published August 2, 2010

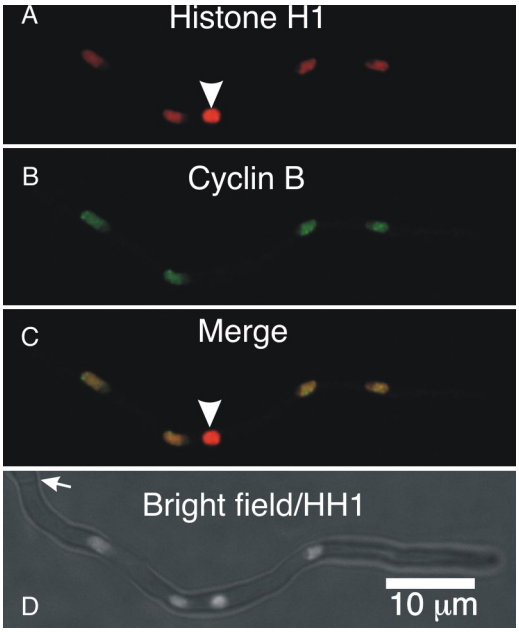

Figure 3. ***MipA*D159 causes a failure of cyclin B accumulation.** (A–D) A strain carrying *mipA*D159 was grown at a restrictive temperature of 25°C and imaged by spinning-disk confocal microscopy. Projections of z-series stacks are shown, except the brightfield image, which is a single-focal plane, combining brightfield and histone H1 fluorescence, showing the positions of nuclei (the tip-most nucleus is nearly out of the plane of focus) and the septum (arrow). All nuclei are in the same cell. Four have accumulated cyclin B, whereas one (arrowheads) has not. The chromatin in the CB− nucleus appears slightly condensed, as is often the case with these nuclei.

asked whether CB− nuclei resulted from disappearance of cyclin B at an inappropriate time or from failure of cyclin B to accumulate in interphase. Observations of 359 mitoses from many time-lapse datasets revealed that the latter was the case. Nuclei went through mitosis, often showing no mitotic abnormalities, and one or, less frequently, both daughter nuclei failed to accumulate cyclin B in the subsequent interphase (Fig. 5). Although the first nuclear division upon germination rarely resulted in CB− daughter nuclei, the percentage of daughter nuclei that became CB− increased with each successive round of mitosis until the majority of mitoses produced at least one CB− daughter nuclei (Fig. 6). Other than the increase over time, there was no obvious pattern with respect to nuclei becoming CB−.

From the same time-lapse datasets, we found that CB− nuclei did not go through mitosis or accumulate cyclin B in subsequent cell cycles. In effect, the CB− nuclei were removed from the cell cycle. When other nuclei in the same cell entered mitosis, releasing cyclin B into the cytoplasm, a small amount of cyclin B entered CB− nuclei (because of partial disassembly of the NPC; see the following sections) but quickly disappeared. The chromatin partially condensed as the cyclin B entered and decondensed as it disappeared. Observations of histone H1–mRFP revealed that CB− nuclei did not become grossly polyploid over time as other nuclei in the same cells passed through multiple cell cycles, although we cannot rule out the possibility that some DNA replication may have occurred. The combination of increasing percentages of daughter nuclei becoming CB− after each round of mitosis and the fact that once nuclei become CB− they stay CB− results in an increase in CB− nuclei over time (Fig. S2) that must contribute significantly to growth inhibition.

In combination, these data indicate that *mipA*D159 causes a failure of accumulation of cyclin B in interphase at restrictive temperatures, and this implies that γ-tubulin has an important, previously undiscovered function in the nuclear accumulation of cyclin B. Because different nuclei in the same cell exhibit different behaviors with respect to the accumulation of cyclin B, this phenomenon is nuclear autonomous and does not lend itself to bulk biochemical analysis. Consequently, we have performed observational and molecular genetic experiments to try to understand this phenomenon.

Failure of cyclin B accumulation is not simply because of abnormal mitosis

*Mip*AD159 causes multiple mitotic defects at restrictive temperatures, including chromosomal nondisjunction (Prigozhina et al., 2004). Consequently, we asked whether the failure of nuclei to accumulate cyclin B was simply a result of defective chromosomal segregation. As mentioned above, time-lapse observations of LO1439 revealed that when nuclei underwent apparently normal mitosis, one of the two daughter nuclei often failed to accumulate cyclin B in the subsequent interphase (Fig. 5). Conversely, many aneuploid nuclei accumulated cyclin B normally (Fig. S3). We scored 127 nuclei that were obviously aneuploid (displaying a dramatically different amount of chromatin from *mipA*+ controls, as judged by histone H1–mRFP fluorescence) after incubation at a restrictive temperature of 25°C for 23 h, and 63 of them accumulated cyclin B. Thus, the failure of accumulation of cyclin B is not an obligate consequence of abnormal chromosomal segregation.

The failure of cyclin B accumulation is not a general nuclear transport defect

To determine whether nuclei fail to accumulate cyclin B because of a general nuclear transport defect, we constructed a strain (LO2589) carrying *mipA*D159, cyclin B–GFP, and the *stuA* nuclear localization signal fused to DsRed fluorescent protein (NLS-DsRed; Suelmann et al., 1997) under the control of the constitutive *gpd* promoter (Toews et al., 2004). At the restrictive temperature, NLS-DsRed accumulated in all nuclei, including those that failed to accumulate cyclin B–GFP (Fig. 7). Nuclei that are defective in cyclin B accumulation are, thus, capable of nuclear transport.

These data indicate that NPCs are functional in CB− nuclei. To observe the behavior of NPCs directly, we created a strain (LO1668) carrying *mipA*D159, cyclin B–GFP, and a functional fusion of the *A. nidulans* homologue of the NPC protein nup49 with mCherry (Osmani et al., 2006; De Souza and Osmani, 2007). Nup49-mCherry was present at the nuclear envelope of both CB+ and CB− interphase nuclei (Fig. S4 A). When cells entered mitosis, nup49-mCherry dissociated from CB− nuclei at the same time that it dissociated from normal nuclei. After mitosis, nup49-mCherry relocalized to the nuclear envelopes of nuclei that remained CB− through the following cell cycle. Thus, nuclear pore assembly and disassembly appear to be normal in CB− nuclei.

Published August 2, 2010

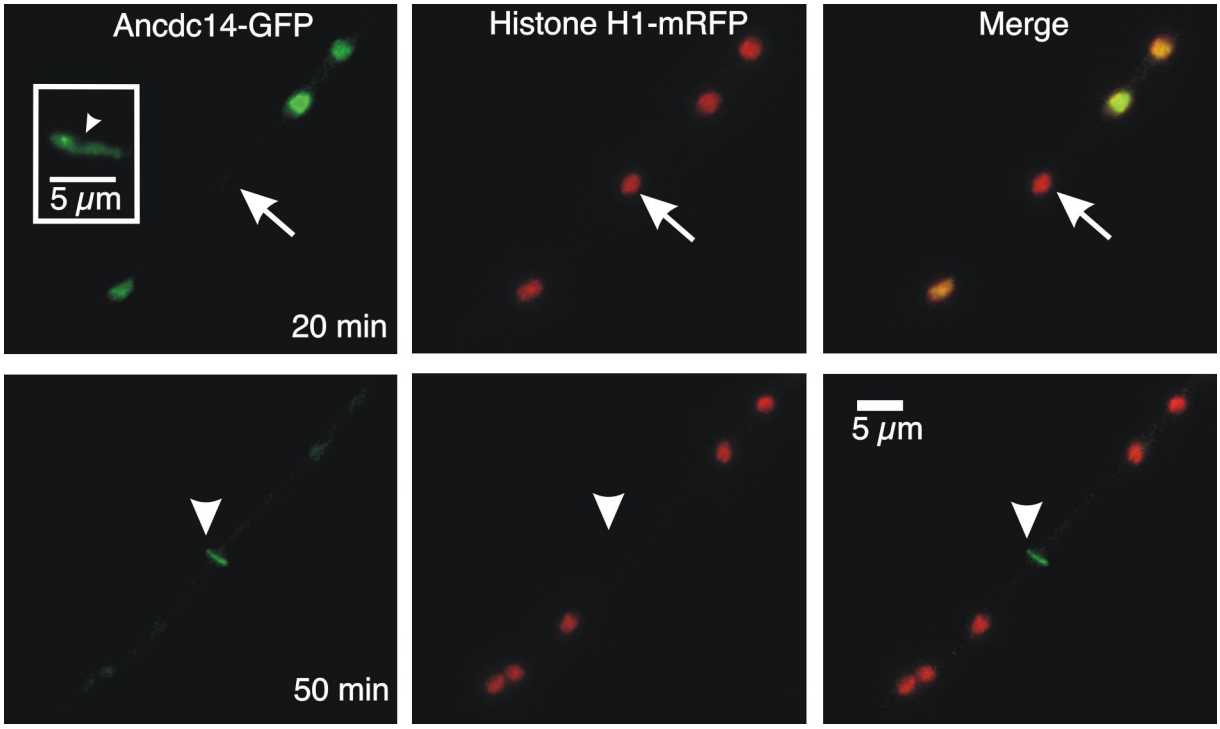

Figure 4. **Ancdc14 localization.** (top left) The inset shows Ancdc14-GFP in a wild-type strain. The empty region (arrowhead) is the nucleolus. The remaining images are projections of the 20- and 50-min time points from a set of z-series stacks collected at 10-min intervals of a strain carrying *mip*AD159 grown at a restrictive temperature of 25°C. At t = 20 min, one nucleus (arrows) has not accumulated a significant amount of Ancdc14 even though other nuclei in the same cell have accumulated the protein. Mitosis occurred between the 20- and 30-min time points, and at the 50-min time point, all nuclei have little Ancdc14, but Ancdc14 does localize to the forming septum (arrowheads).

These data cast light on the control of nuclear pore disassembly at mitotic onset. Nuclear pore disassembly could, in principle, be controlled by an internal signal generated by G_2 nuclei as they enter mitosis. Because CB− nuclei do not cycle, it is unlikely that they generate a normal nuclear pore disassembly signal. Rather, these results suggest that nuclear pore disassembly is controlled by a cytoplasmic signal that passes through the cell.

Cyclin B is normally exported from nuclei via a CRM1-mediated pathway (Kornbluth et al., 1992; Hagting et al., 1998; Yang et al., 1998). To determine whether CB− nuclei fail to accumulate cyclin B because they constitutively export it, we created strain LO2994 that carries cyclin B–GFP, *mip*AD159, histone H1–mRFP, and the *crmA*T525C allele. The *crmA* gene of *A. nidulans* encodes a CRM1 homologue, and the mutation *crmA*T525C makes the protein sensitive to leptomycin B such that 10 ng/ml of the compound prevents CRM1-mediated export (Todd et al., 2005). We grew LO2994 at 25°C to allow the accumulation of CB− nuclei, then added leptomycin B and observed CB− nuclei by time-lapse microscopy to determine whether they accumulated cyclin B–GFP. CB− nuclei did not accumulate cyclin B–GFP in treatments with 10, 20, or even 100 ng/ml leptomycin B (Fig. S4 B). Thus, constitutive export via the CRM1 pathway is not responsible for CB− nuclei.

The cyclin B accumulation defect is caused by failure of APC/C inactivation

Many of the defects caused by *mip*AD159 at restrictive temperatures (Prigozhina et al., 2004) are consistent with *mip*AD159 causing misregulation of APC/C. The APC/C is a ubiquitin ligase that ubiquitinates key mitotic regulatory proteins, targeting them for destruction. Activation of the APC/C is required for exit from mitosis, and it remains active through G_1 to prevent accumulation of cyclins and other substrates (for review see van Leuken et al., 2008). The APC/C is normally inactivated at the G_1/S transition and stays inactive until all kinetochores are attached to spindles in a bipolar fashion, and the spindle assembly checkpoint (SAC) is inactivated (Buschhorn and Peters, 2006; for review see Acquaviva and Pines, 2006). Cyclin B is an APC/C target, and CB− nuclei could, in principle, be caused by nuclear autonomous failure of APC/C inactivation.

The APC/C targets cyclin B for destruction by recognizing a conserved motif near the N terminus called the destruction box (Glotzer et al., 1991; Glotzer, 1995). N-terminal truncations deleting the destruction box result in a form of cyclin B that binds to Cdk1 and drives the cell cycle, but because it is no longer targeted by the APC/C, it is not destroyed in mitosis and causes a mitotic arrest (Murray et al., 1989; Glotzer et al., 1991; Glotzer, 1995; De Souza et al., 2009; for review see Acquaviva and Pines, 2006). *A. nidulans* cyclin B has a canonical destruction box (RAALGDVSN) near its N terminus. We created a truncated version of cyclin B–GFP lacking the N-terminal 73 amino acids that contain the destruction box–deleted cyclin B–GFP (dbΔ–cyclin B–GFP). Because destruction of cyclin B is essential for the completion of mitosis, expression of dbΔ–cyclin B–GFP should prevent mitotic exit and thus be lethal.

Published August 2, 2010

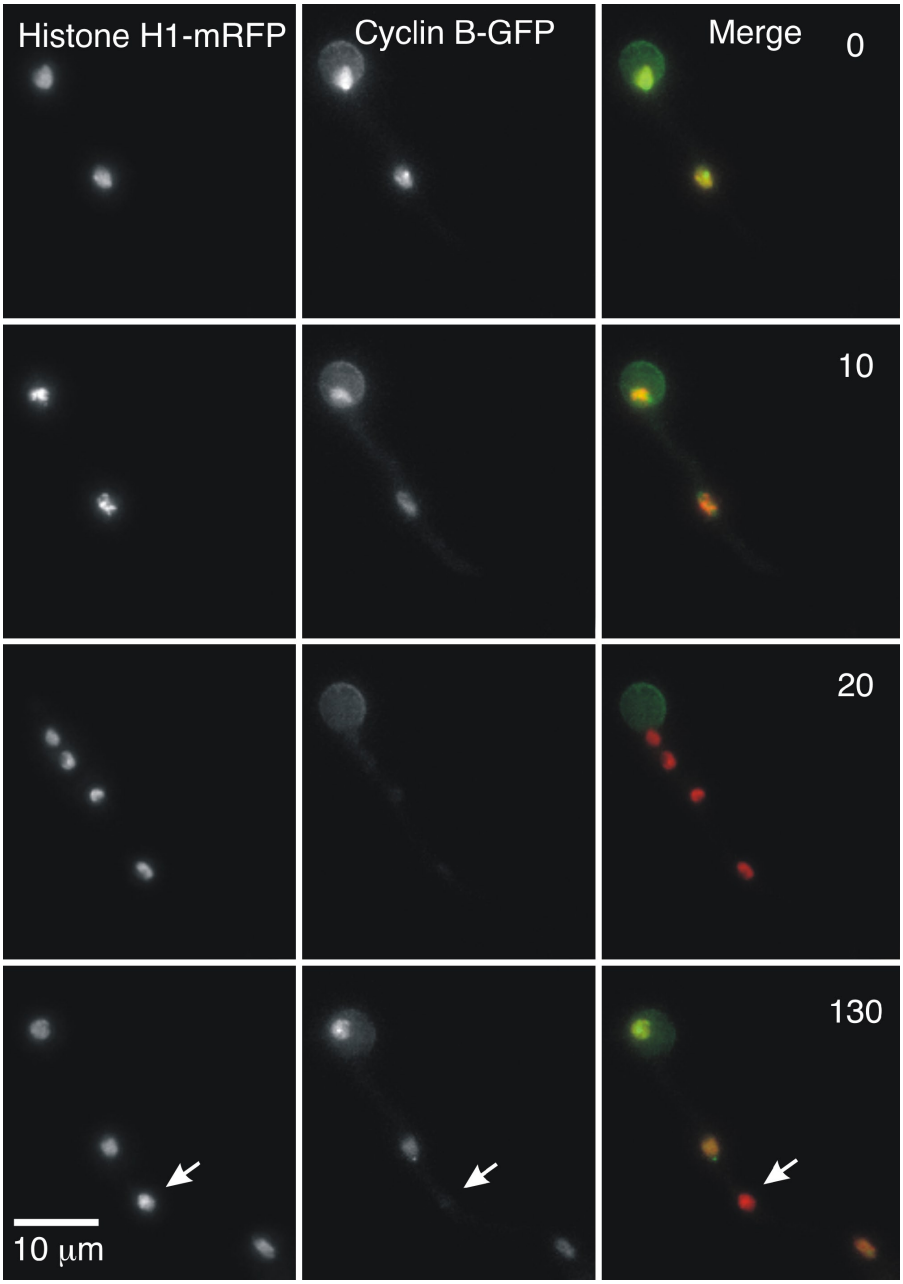

Figure 5. **CB− nuclei are caused by the failure of cyclin B accumulation in interphase.** Images are projections from a set of z-series stacks collected at 10-min intervals (time of collection at the top right of the merge panels). At t = 0, two nuclei in the same cell are in G_2. The conidium that germinated to form the germling shown exhibits autofluorescence at the GFP wavelength. At t = 10 min, the nuclei are in mitosis. At t = 20 min, the nuclei have divided normally and have entered G_1. As in controls, the nuclei lack cyclin B. At t = 130 min, cyclin B has begun to accumulate in three nuclei but not in the fourth (arrows).

To overcome this problem, we placed dbΔ–cyclin B–GFP under the control of the highly regulatable *alcA* promoter (Waring et al., 1989). We integrated the construct into the *wA* (white spore color) locus of a strain carrying histone H1–mRFP, leaving the wild-type copy of the *nimE* (cyclin B) gene intact. The resulting strain, LO1847, grew like the parent on *alcA*-repressing media, but under inducing conditions, growth was severely inhibited (Fig. 8 A), indicating that expression of dbΔ–cyclin B–GFP was efficiently repressed on glucose and efficiently induced under inducing conditions.

We next examined the effects of dbΔ–cyclin B–GFP microscopically. Upon induction, dbΔ–cyclin B–GFP gradually accumulated in nuclei. Consistent with recent results using a slightly different destruction box–deleted cyclin B construct (De Souza et al., 2009), nuclei in cells expressing dbΔ–cyclin B–GFP entered mitosis and progressed through anaphase, but the dbΔ–cyclin B–GFP signal was visible at spindle poles for an extended period, and nuclei were blocked in telophase.

To determine the effects of *mipA*D159 on dbΔ–cyclin B–GFP accumulation, we created a strain (LO1849) that carries dbΔ–cyclin B–GFP, histone H1–mRFP, and *mipA*D159. We also created control strains LO1943 (wild-type cyclin B–GFP under the control of the *alcA* promoter integrated at the *wA* locus, histone H1–mRFP, and *mipA*D159), LO1439 (*mipA*D159, cyclin B–GFP, and histone H1–mRFP), and LO1438 (*mipA*+, cyclin B–GFP, and histone H1–mRFP).

Conidia were incubated in medium containing glucose to repress dbΔ–cyclin B–GFP expression at a permissive temperature of 37°C for 12 h. The repressing medium was washed out and replaced with inducing medium, and the culture was immediately

Published August 2, 2010

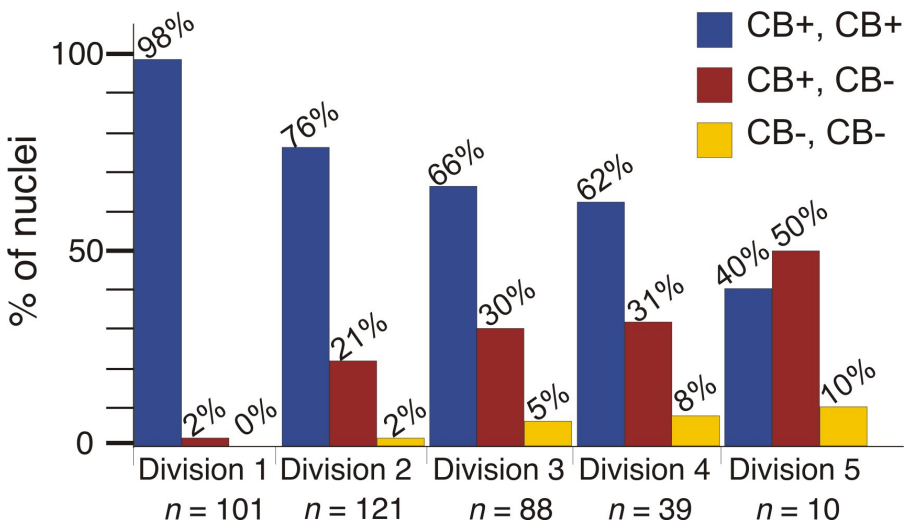

Figure 6. **Increase in the percentage of CB− nuclei after each round of mitosis.** Division 1 is the first division after germination, etc. CB+, CB+ indicates that both daughter nuclei from a mitosis accumulated cyclin B in the following interphase; CB+, CB− indicates that one accumulated cyclin B; and CB−, CB− indicates that neither accumulated cyclin B. The *n* values indicate the number of nuclei scored for each round of division.

shifted to a restrictive temperature of 25°C. Cells were imaged 1–3 h after the shift. This time window was chosen because it is less than one cell cycle after induction but long enough after induction to allow cyclin B–GFP or dbΔ–cyclin B–GFP to accumulate in nuclei. As shown in Fig. 8 B, deletion of the destruction box allowed cyclin B to accumulate in nearly all nuclei. The accumulation was not because of alterations of expression levels by the alcA promoter because cells expressing wild-type cyclin B–GFP under control of this promoter contained many CB− nuclei.

To verify these results, we created a strain (LO1910) that carries *mip*AD159 and dbΔ–cyclin B–GFP under the control of the *alcA* promoter along with wild-type cyclin B–mCherry under the control of its endogenous promoter. We performed a temperature-shift dbΔ–cyclin B–GFP induction experiment as above and found that all nuclei accumulated dbΔ–cyclin B–GFP, but a subset of these nuclei did not accumulate cyclin B–mCherry (Fig. 8 C). Thus, two separate sets of experiments reveal that the removal of the destruction box targeted by the APC/C overrides the cyclin B accumulation defect caused by *mip*AD159. It follows that the cyclin B accumulation defect caused by *mip*AD159 is because of inappropriately active APC/C. γ-Tubulin, thus, plays an important role in inactivating the APC/C in interphase, an activity that is compromised in *mip*AD159.

The activity of the APC/C can be reset in CB− nuclei

Our data indicate that *mip*AD159 causes a nuclear autonomous failure of APC/C inactivation. If this is correct, inactivation of the APC/C in those nuclei should cause them to be reset to become CB+. Treatment with antimicrotubule agents activates the SAC, which, in turn, inactivates the APC/C (Hoyt et al., 1991; Li and Murray, 1991; for review see Musacchio and Salmon, 2007). It follows that if *mip*AD159 causes constitutive activation of the APC/C, prolonged treatment with an antimicrotubule agent might inactivate the APC/C, allowing some nuclei to reset and accumulate cyclin B.

Benomyl at a concentration of 2.4 μg/ml completely depolymerizes microtubules (Horio and Oakley, 2005). When wild-type cells treated with benomyl enter mitosis, the mitotic spindle does not form, and nuclei are arrested in mitosis for an extended period with an activated SAC. Eventually, the SAC becomes inactivated, and nuclei exit mitosis and enter the next cell cycle (unpublished data). These nuclei accumulate cyclin B normally in interphase and are able to synthesize DNA and

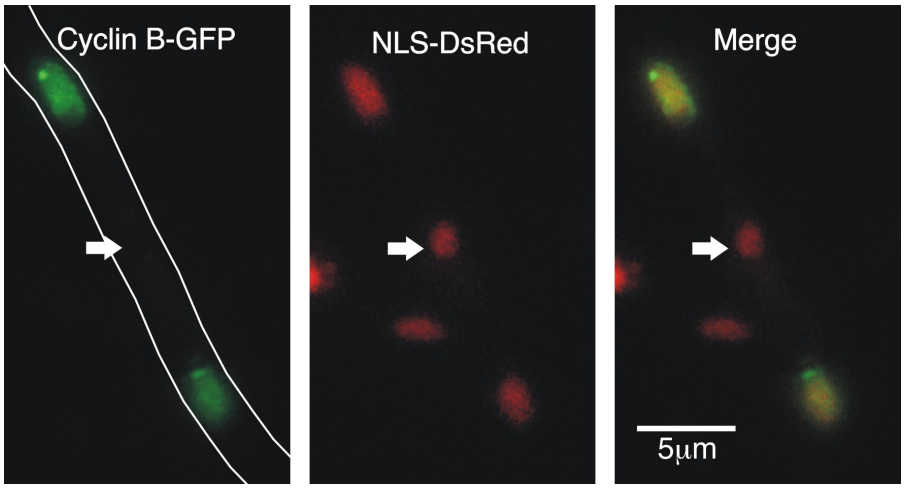

Figure 7. **CB− nuclei are not defective for nuclear import.** Images are projections of z-series stacks of the same field. Portions of two hyphae are shown, and one hypha containing three nuclei is outlined in the cyclin B–GFP panel. In this hypha, the central nucleus (arrows) is CB− but has taken up NLS-DsRed.

Published August 2, 2010

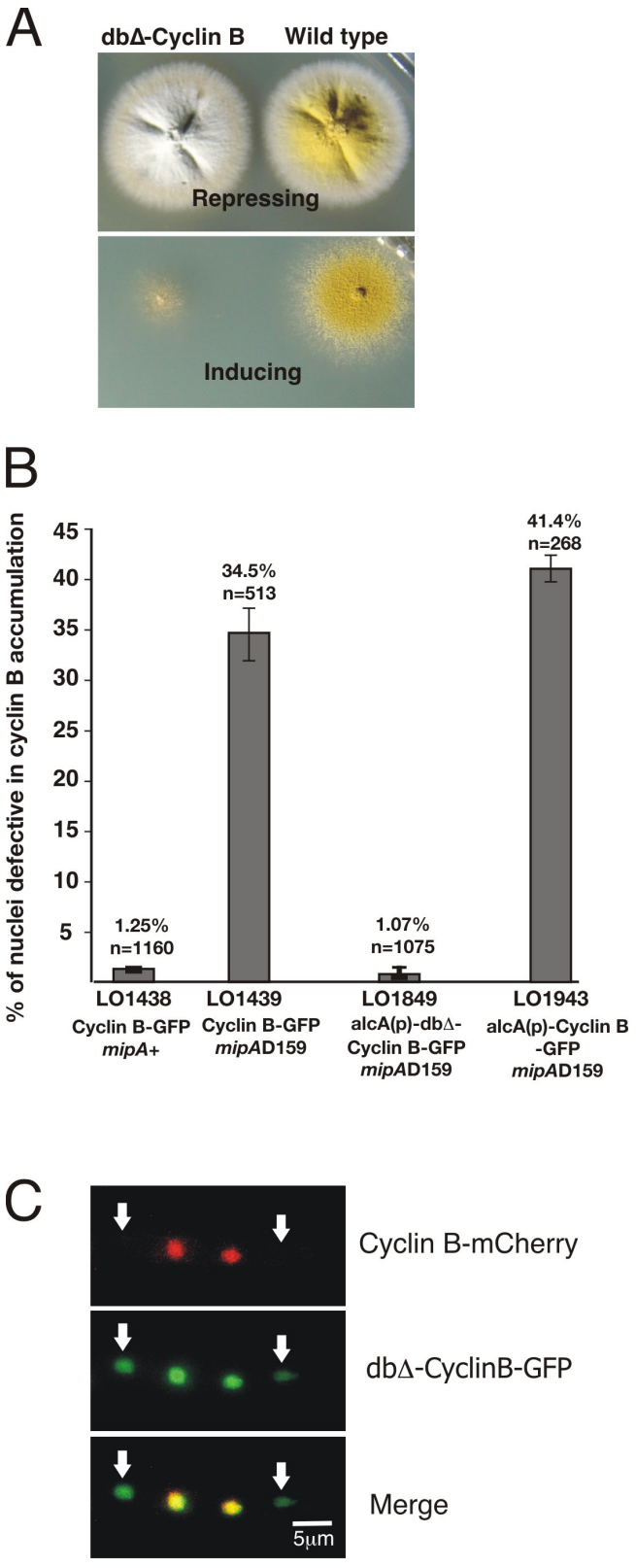

Figure 8. **CB− nuclei are caused by constitutive APC/C activity.** (A) Growth of a strain carrying dbΔ–cyclin B–GFP under the control of the *alcA* promoter integrated at the white (*wA*) locus and a wild-type control. On a medium that represses the *alcA* promoter, the strain carrying the dbΔ–cyclin B–GFP construct grows normally, reflecting the fact that very little dbΔ–cyclin B–GFP is made. On medium that induces expression from the *alcA* promoter, the dbΔ–cyclin B–GFP strain is severely inhibited for growth, reflecting the fact that expression of the destruction box–deleted cyclin B inhibits growth. (B) dbΔ–cyclin B–GFP accumulates in all nuclei. Spores were incubated at a permissive temperature (37°C) for 12 h and shifted to a restrictive temperature (25°C). Cells were imaged 1–3 h after the shift. The percentage of CB− nuclei was scored in tip cells in which at least one nucleus had visibly accumulated cyclin B. In a strain carrying wild-type cyclin B–GFP and the wild-type γ-tubulin allele (*mipA*+), CB− nuclei were very rare. In a strain with wild-type cyclin B–GFP and *mipA*D159, 34.5% of nuclei were CB−. In a strain carrying *mipA*D159 and dbΔ–cyclin B–GFP, CB− nuclei were very rare, but they were abundant in a strain carrying wild-type cyclin B–GFP under the control of the *alcA* promoter. (C) A strain carrying a wild-type cyclin B–mCherry construct and dbΔ–cyclin B–GFP, under the control of the *alcA* promoter, were grown at a permissive temperature in *alcA*-repressing media and shifted to an inducing medium at a restrictive temperature. All four nuclei are in the same cell. dbΔ–cyclin B–GFP accumulates in all nuclei, but two nuclei (arrows) have not accumulated the wild-type cyclin B–mCherry. Error bars indicate mean ± SD.

increase in ploidy but do not divide during mitosis. We grew a strain carrying *mipA*D159 at the restrictive temperature of 25°C to accumulate CB− nuclei. After addition of benomyl, we imaged hyphae over 5–10 h to determine whether CB− nuclei regained the ability to accumulate cyclin B (Fig. 9). Because benomyl depolymerizes microtubules that are required for nuclear movement, nuclei moved slowly, and this allowed us to follow them over long periods. When cells entered mitosis, a portion of the cyclin B exited from CB+ nuclei, and the chromosomes condensed. During mitotic arrest, CB− nuclei accumulated some cyclin B, reflecting the fact that the nuclei were blocked in a semi-open conformation with much of the NPC disassembled (De Souza and Osmani, 2007). Eventually, cyclin B disappeared completely from all nuclei (presumably caused by APC/C activation at the end of the block), and nuclei exited mitosis. We followed 71 nuclei by time-lapse microscopy through interphase, mitosis, and at least one subsequent interphase. 23 nuclei (32%) that were CB+ before mitosis remained CB+ through the following interphase. 20 nuclei (28%) that were CB− became CB+, indicating that CB− nuclei can indeed be reset to be CB+ by a prolonged mitotic arrest. 16 nuclei (23%) that were CB− remained CB−. Interestingly, 12 nuclei (17%) that were CB+ became CB−, showing that *mipA*D159 can cause nuclei to become CB− in the absence of microtubules. Importantly, the fact that nuclei can become CB− when microtubules are depolymerized appears to rule out the possibility that CB− nuclei are related to any potential microtubule nucleation defects of *mipA*D159. It is also worth noting that no nuclei changed from CB− to CB+ or vice versa until the cell had entered and exited mitosis. In control experiments with a *mipA*+ strain, the great majority of nuclei (80/85; 94.1%) remained CB+ throughout the experiment, but a small fraction (5/85; 5.9%) became CB−. Although this number is much lower than in the strain carrying *mipA*D159, it is intriguing and worthy of further study.

The APC/C is a potential source of nuclear autonomy

In the absence of benomyl, once nuclei become CB−, they remain CB−. If CB− nuclei are caused by a constitutively active APC/C, it follows that the APC/C in nuclei should not

Published August 2, 2010

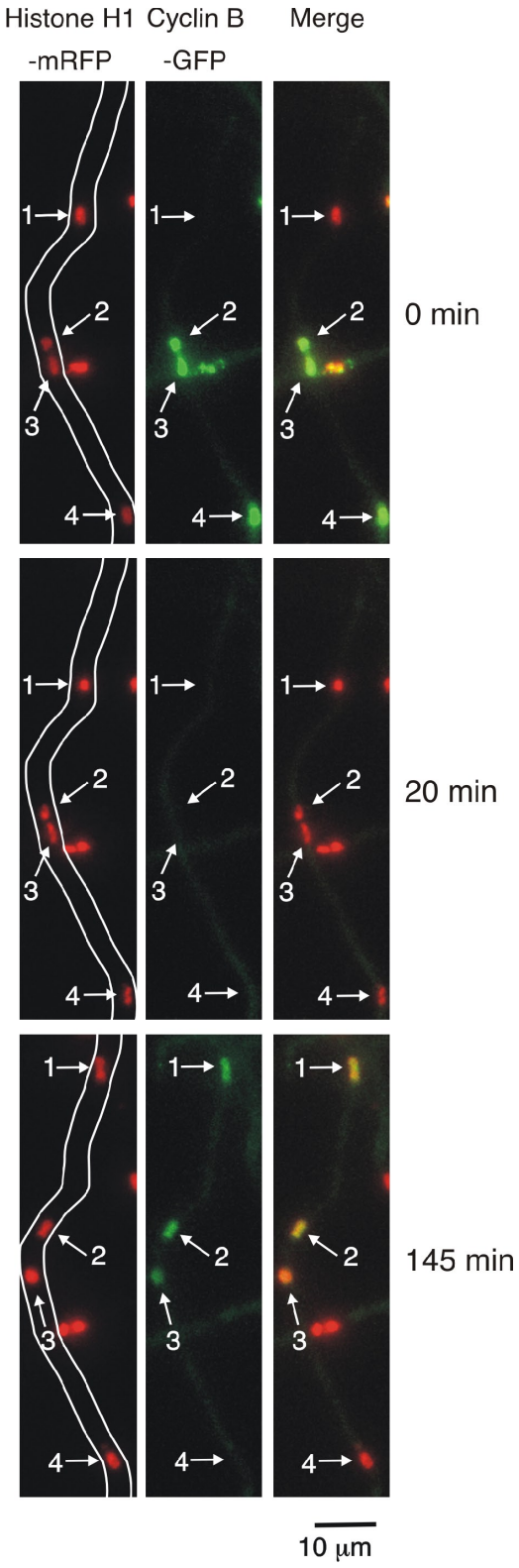

Figure 9. **Benomyl causes CB− nuclei to reset.** The images shown are z-axis projections of a strain carrying *mipA*D159 taken from a time-lapse dataset collected at 25°C. The four nuclei (arrows) are in the same cell (left, hypha is outlined). At t = 0, nucleus 1 is CB−, and the others are CB+. At t = 20 min, the nuclei have gone through mitosis (although no nuclear division occurred because of the absence of spindles), and cyclin B is absent from all nuclei. At t = 145 min, cyclin B has accumulated in nucleus 1, which was formerly CB−, but is absent from nucleus 4, which was previously CB+. Nuclei 2 and 3 are CB+ before and after the division.

exchange freely with APC/C in the cytoplasm nor leave the nucleus completely at any time in the cell cycle. To determine whether the localization pattern of the APC/C is consistent with a constitutively active APC/C causing CB− nuclei, we wished to tag and image at least one APC/C component. It is notoriously difficult to obtain functional tagged versions of APC/C components (Acquaviva et al., 2004), but we were able to create a functional tagged version of the *A. nidulans* APC3 homologue BimA (O'Donnell et al., 1991; Ye et al., 1998). The localization of BimA has previously been studied by immunofluorescence microscopy (Mirabito and Morris, 1993), where it was reported to localize to SPBs or, if overexpressed, to the nucleus. Although we did see an apparent SPB localization in some nuclei, the predominant localization of BimA-GFP was with chromatin. BimA was nuclear in interphase and early mitosis, and during anaphase, BimA-GFP localized to the separating chromosomes and the spindle between the separating chromosomes (Fig. 10). It then disappeared from the spindle but remained associated with the decondensing chromatin. Thus, BimA is not freely diffusible, and its continuous association with chromatin suggests that it could be a source of nuclear autonomy.

A question that arises is why the localization pattern we have observed is different from the pattern observed by immunofluorescence. *BimA* is an essential gene (O'Donnell et al., 1991), and our *bimA*-GFP construct appears fully functional in that it is the only copy in the genome and supports normal growth and doesn't cause any obvious mitotic abnormalities. It is expressed from its endogenous promoter and, thus, should be present at normal levels. Therefore, we are confident that the localization pattern we have observed accurately reflects the distribution of BimA in the cell.

We next asked whether BimA-GFP localizes to all nuclei in a strain carrying *mipA*D159 at the restrictive temperature of 25°C. For this, we grew strain LO3935 at 25°C for 23 h. Under these conditions, 39.5% of nuclei did not accumulate cyclin B. In contrast, 96.6 ± 1.3% of nuclei contained visible BimA-GFP (mean and SD of three experiments; total $n = 634$). These data indicate that most if not all CB− nuclei contained BimA and, by inference, APC/C.

Discussion

At restrictive temperatures, in strains carrying the γ-tubulin mutation *mipA*D159, a subset of nuclei fails to accumulate the key regulatory proteins cyclin B and Cdk1 and the phosphatase Ancdc14, whereas other nuclei in the same cells accumulate them normally. Because Cdk1 localization depends on cyclin B, we presume that the failure of accumulation of Cdk1 is a consequence of the failure of accumulation of cyclin B. In the absence of the Cdk1–cyclin B complex, which is required for progression through both S and M phases in *A. nidulans* (Osmani et al., 1994), nuclei are effectively removed from the cell cycle. Additional nuclei become CB− in every cell cycle, resulting in an increase over time in the percentage of nuclei that are CB−, thus contributing to growth inhibition.

Our results strongly indicate that CB− nuclei result from a nuclear autonomous failure of inactivation of the APC/C, resulting

Published August 2, 2010

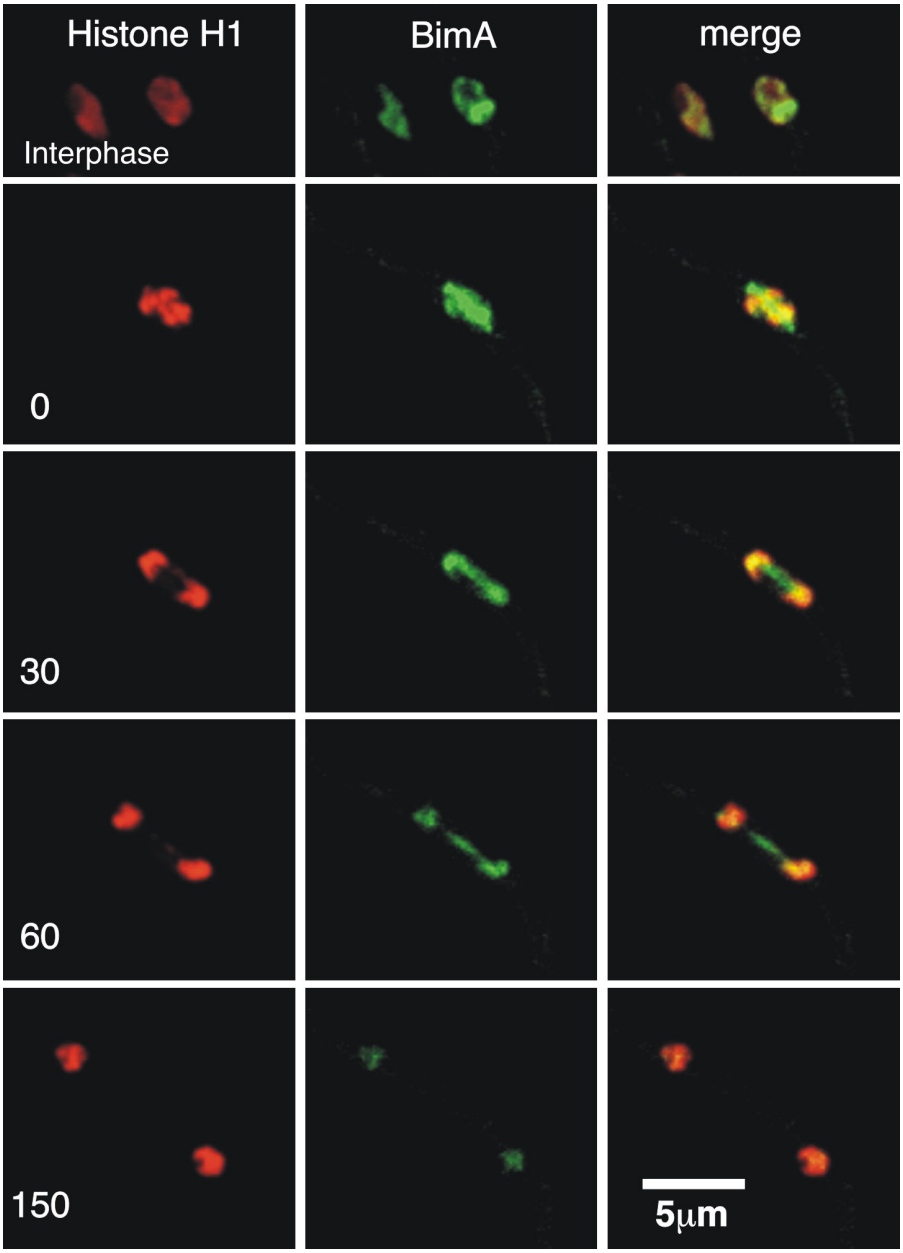

Figure 10. **BimA localization in vivo in a *mipA*+ strain.** All images are projections of z-series stacks acquired with a spinning-disk confocal microscope. In interphase, BimA-GFP localizes to the nucleus but has a slightly different localization pattern in the nucleus from the chromatin visualized with histone H1–mCherry. Mitotic images are from a time-lapse dataset acquired with a spinning-disk confocal microscope (not the same field as the interphase image). (left) Time of acquisition (s) is shown. BimA localizes to chromatin and the spindle and disappears from the spindle in telophase. At the 150-s time point, BimA is faint because of photobleaching.

in the continuous targeting of cyclin B for proteolysis. The lack of Ancdc14 in CB− nuclei is also consistent with a permanently active APC/C because Ancdc14 has a canonical destruction box and is thus likely to be an APC/C target. Because a γ-tubulin mutation causes a failure of inactivation of the APC/C at restrictive temperatures, it follows that γ-tubulin normally plays an important role in the inactivation of the APC/C.

The APC/C, which is active in mitosis, is inactivated before S phase, allowing the accumulation of APC/C substrates (such as cyclin B) that are required for DNA replication and cell cycle progression (for review see Acquaviva and Pines, 2006). Our observations show that CB− nuclei result from formerly CB+ nuclei that enter and exit mitosis but do not subsequently accumulate cyclin B. It follows that the failure of APC/C inactivation occurs after mitotic APC/C activation but before S when cyclin B accumulation normally becomes apparent.

Our benomyl data allow us to draw two important conclusions. The first is that because some CB− nuclei are reset in benomyl to become CB+, CB− nuclei are not biochemically dead. They have the potential to cycle but are prevented from doing so by the constitutively active APC/C. The second is that because CB+ nuclei can become CB− in the absence of microtubules, the failure of inactivation of the APC/C by *mipA*D159 is independent of microtubules and is not a consequence of any microtubule nucleation defect that might be caused by *mipA*D159. One question that arises is why some nuclei are reset to become CB+, whereas others are not. Our data do not allow us to answer this question definitively. One possibility is that the APC/C is not completely inactivated in some nuclei for reasons that are not clear but might, for example, relate to the amount of active APC/C in each particular nucleus. Another is that the APC/C is inactivated in mitosis in each nucleus but subsequently becomes

Published August 2, 2010

reactivated in some nuclei in a probabilistic fashion after mitotic exit such that cyclin B does not accumulate. Some nuclei that are CB− would thus remain CB− even though the APC/C had been transiently inactivated during mitotic blockage.

These data raise the question of why the SAC does not inactivate the APC/C in CB− nuclei when they enter mitosis in the absence of benomyl. One possibility is that the activation of the SAC requires Cdk1 activity (D'Angiolella et al., 2003; Wong and Fang, 2007), which is missing in CB− nuclei. Another is that one or more SAC proteins are destroyed by the constitutively active APC/C. In either case, a prolonged mitotic block would likely allow enough protein exchange to restore SAC activity.

Why do only a fraction of the nuclei become CB− after each round of nuclear division? *Mip*AD159 is a recessive allele (Jung et al., 2001). It is therefore likely to be a loss of function allele, but loss of a subset of γ-tubulin functions rather than all functions because microtubules are nucleated in abundance in strains carrying *mip*AD159 (Jung et al., 2001). The simplest explanation is that the function of γ-tubulin in inactivating the APC/C is reduced but not eliminated in *mipAD*159, and this leads to a stochastic loss of APC/C inactivation in each G_1 rather than a certain loss.

γ-Tubulin, the centrosome, and cell cycle regulation

Our data provide the first evidence that γ-tubulin plays a role in inactivation of the APC/C after mitotic exit. Evidence is accumulating that the γ-tubulin complex and polar microtubule-organizing centers, the SPB and the centrosome, play an important role in cell cycle regulation (Vardy and Toda, 2000; Sluder, 2005; Müller et al., 2006; Mikule et al., 2007; Cheng et al., 2008; for review see Cuschieri et al., 2007). It is also becoming clear that cyclin B destruction is spatially regulated in phylogenetically distant organisms and that polar microtubule-organizing centers may play a role in this spatial regulation (Fig. 1 B; Huang and Raff, 1999; Wakefield et al., 2000; De Souza et al., 2009). Also note that the patchy distribution of cyclin B that we see in some *mip*AD159 mitotic nuclei (Fig. S1) may reflect abnormal spatial regulation of cyclin B destruction. Given these facts and the fact that the γ-tubulin encoded by the *mip*AD159 allele localizes normally to the SPB (Jung et al., 2001), it is reasonable to assume that the function of γ-tubulin in inactivating the APC/C occurs at the SPB. For example, it could hypothetically be involved in a signal transduction pathway that senses mitotic and cell cycle events and inactivates the APC/C after mitosis. However, our data are also consistent with γ-tubulin functioning away from the SPB. For example, a small amount of γ-tubulin (or γ-tubulin small complexes) independent of the SPB could, in principle, interact directly with the APC/C and be involved in its inactivation.

BimA localization and nuclear autonomy

In some fungi, all nuclei in a cell go through mitosis in synchrony, whereas in others, mitosis and the cell cycle are nuclear autonomous. Our data reveal that although nuclei in *A. nidulans* normally go through the cell cycle in synchrony, when perturbed by *mip*AD159, they can behave in an autonomous fashion. Moreover, the localization pattern of BimA suggests that the APC/C is a potential source of nuclear autonomy.

Materials and methods

Strains

Table S1 shows a complete list of the strains used in these experiments and their genotypes.

Microscopy

For imaging, conidia were inoculated into liquid minimal medium (6 g/liter $NaNO_3$, 0.52 g/liter KCl, 0.52 g/liter $MgSO_4$ $7H_2O$, 1.52 g/liter KH_2PO_4, 10 g/liter D-glucose, and 1 ml/liter of a trace element solution [Vishniac and Santer, 1957], pH adjusted to 6.5, with NaOH before autoclaving, supplemented as appropriate for nutritional markers) in four- or eight-chamber cover glasses (Lab-Tek; Thermo Fisher Scientific). We used three systems for imaging. Two were inverted microscopes (IX71; Olympus) equipped with shutters, filter wheels, z-axis drives (Prior Scientific), and mercury light sources. One was equipped with an ORCA ER camera (Hamamatsu Photonics) and the other with an ORCA ERAG camera (Hamamatsu Photonics). We used Semrock GFP/DsRed2X2M-B dual-band Sedat filter sets (459–481-nm bandpass excitation filter for GFP and a 546–566-nm excitation filter for mCherry and mRFP), dual-reflection band dichroic (457–480- and 542–565-nm reflection bands; 500–529- and 584–679-nm transmission bands), and two separate emission filters (GFP, 499–529 nm; mCherry and mRFP, 580–654 nm) were used. Images were acquired with a 60× 1.42 NA Plan Apochromatic objective (Olympus) using Slidebook (Intelligent Imaging Innovations) or Volocity software (PerkinElmer) installed on computers (PowerMac; Apple). For time-lapse two-channel imaging of live cells, z-series stacks were collected at each time point, and maximum intensity projections from all time points were combined to generate videos using Slidebook or Volocity software. The third system was a spinning-disk confocal system (UltraVIEW VoX; PerkinElmer) mounted on an inverted microscope (IX71; Olympus). It was equipped with an environmental chamber to maintain stable temperatures and a software-controlled piezoelectric stage for rapid z-axis movement. Solid-state 488- and 561-nm lasers were used for excitation. A 60× 1.42 NA objective (Olympus) was used (in some cases with a 1.6× Optovar), and images were collected with an ORCA ERAG camera. The system was controlled by a computer (PowerMac) running Volocity software.

To prepare figures, images were exported directly from the imaging software after adjustment of minimum and maximum intensity levels. No γ adjustments were made. Graphic Converter was used to change the file format of some images. Figures were drawn and/or assembled with CorelDraw software.

Gene targeting and transformation

Transformation procedures and generation of linear transforming molecules by fusion PCR were performed as described previously (Nayak et al., 2006; Szewczyk et al., 2006). To create C-terminal fluorescent protein fusions, the linear transforming molecule consisted of ∼500- or 1,000 bp of the coding sequence of the target gene fused in frame to a glycine–alanine linker (Yang et al., 2004), which was in turn fused in frame with the fluorescent protein coding sequence (either GFP, mCherry, or mRFP). The fusion protein coding sequence was followed by a selectable marker (*A. fumigatus pyrG* [*AfpyrG*; Weidner et al., 1998], *A. fumigatus riboB* [*AfriboB*; Nayak et al., 2006], or *A. fumigatus pyroA* [*AfpyroA*; Nayak et al., 2006]), which was in turn followed by ∼500 or 1,000 bp of 3′ untranslated region flanking the target gene. Integration of such fragments by homologous recombination resulted in a single copy of the gene (the only copy in the genome) under the control of its native promoter and fused in frame to the fluorescent protein coding sequence. The GFP variant we used was a plant-adapted GFP (Fernández-Abalos et al., 1998) that works particularly well in *A. nidulans*. mRFP and mCherry were used as previously described (Campbell et al., 2002; Shaner et al., 2004; Toews et al., 2004). Correct gene targeting was facilitated by the use of *nkuAΔ* strains (Nayak et al., 2006).

The dbΔ–cyclin B–GFP construct was created as follows. A fragment of the cyclin B gene extending from nucleotide 316 to the stop codon (nucleotide 1,672) was amplified by PCR. This fragment excludes the N-terminal 73 amino acids that contain the destruction box (bp 285–312). The primers used to amplify this fragment were designed with a tail at the 5′ end that annealed to the *alcA* promoter, including a start codon, and

Published August 2, 2010

a tail at the 3′ end that annealed to a GFP-*AfpyrG* cassette. We also amplified regions flanking the *wA* gene (5′, 996 bp; 3′, 1,007 bp). One of the two primers used to amplify the 5′ flank had a tail that allowed annealing to the *alcA* promoter fragment. One of the primers used to amplify the 3′ *wA* fragment was designed with a tail that allowed annealing to the GFP-*AfpyrG* cassette. The fragments were combined, and a single fragment was amplified by fusion PCR. A similar strategy was used to construct a full-length cyclin B gene fused to GFP-*AfpyrG* under control of the *alcA* promoter with *wA* flanking sequences.

The *alcA* promoter is repressed by glucose and induced by several compounds, including threonine. The inducing medium for our observations was 6 g/liter $NaNO_3$, 0.52 g/liter KCl, 0.52 g/liter $MgSO_4$ $7H_2O$, 1.52 g/liter KH_2PO_4, 9 g/liter fructose, and 1 ml/liter of a trace element solution (Vishniac and Santer, 1957) and 6.25 mM threonine. Repressing medium was identical except that it contained 10 g/liter D-glucose instead of fructose and no threonine.

Diagnostic PCR and Southern hybridizations

A. nidulans genomic DNA of transformants was prepared as described previously (Lee and Taylor, 1990). Positive transformants were first confirmed through diagnostic PCR using primers flanking the target sequence. Correct integrations and the absence of extra integrations of transforming DNAs were also verified by Southern hybridizations in dried agarose gels as described previously (Oakley et al., 1987). Radioactively labeled full-length transforming DNA fragments were used as probes.

Inhibitor treatments

LO2994 was grown in minimal medium for 18 h at 25°C before leptomycin B was added to a final concentration of 10 ng/ml. Cells with CB− nuclei were imaged over a period of 3 h after addition of leptomycin B at the restrictive temperature of 25°C. We repeated the experiment with 20 and 100 ng/ml of leptomycin B, imaging up to 15 h after leptomycin B addition, and obtained similar results. Benomyl treatments were performed as previously described (Horio and Oakley, 2005). In brief, benomyl was maintained as a 240 µg/ml solution in 95% ethanol. An appropriate volume of the stock solution was added directly to chambered cover glasses using a micropipeter to give a final concentration of 2.4 µg/ml.

Online supplemental material

Fig. S1 shows abnormal distribution of cyclin B and Cdk1. Fig. S2 shows the accumulation of CB− nuclei in a strain carrying *mip*AD159 over time at a restrictive temperature. Fig. S3 shows aneuploid CB+ nuclei, and Fig. S4 demonstrates that CB− nuclei are not the result of defects in nuclear pore localization or export. Table S1 lists the strains used for these experiments Online supplemental material is available at http://www.jcb.org/cgi/content/full/jcb.201002105/DC1.

We thank Elizabeth Oakley for technical and editorial assistance, Dr. Roger Tsien for the mCherry gene, and Drs. R.B. Todd and M.J. Hynes for the *crmA*T525C mutant.

This work was supported by the National Institutes of Health (grants GM031837 to B.R. Oakley and GM042564 to S.A. Osmani) and the Kansas University Endowment.

Submitted: 18 February 2010
Accepted: 8 July 2010

References

Acquaviva, C., and J. Pines. 2006. The anaphase-promoting complex/cyclosome: APC/C. *J. Cell Sci.* 119:2401–2404. doi:10.1242/jcs.02937

Acquaviva, C., F. Herzog, C. Kraft, and J. Pines. 2004. The anaphase promoting complex/cyclosome is recruited to centromeres by the spindle assembly checkpoint. *Nat. Cell Biol.* 6:892–898. doi:10.1038/ncb1167

Bergen, L.G., and N.R. Morris. 1983. Kinetics of the nuclear division cycle of *Aspergillus nidulans*. *J. Bacteriol.* 156:155–160.

Buschhorn, B.A., and J.M. Peters. 2006. How APC/C orders destruction. *Nat. Cell Biol.* 8:209–211doi:10.1038/ncb0306-209

Campbell, R.E., O. Tour, A.E. Palmer, P.A. Steinbach, G.S. Baird, D.A. Zacharias, and R.Y. Tsien. 2002. A monomeric red fluorescent protein. *Proc. Natl. Acad. Sci. USA.* 99:7877–7882. doi:10.1073/pnas.082243699

Cheng, J., N. Türkel, N. Hemati, M.T. Fuller, A.J. Hunt, and Y.M. Yamashita. 2008. Centrosome misorientation reduces stem cell division during ageing. *Nature.* 456:599–604. doi:10.1038/nature07386

Chesnel, F., F. Bazile, A. Pascal, and J.Z. Kubiak. 2006. Cyclin B dissociation from CDK1 precedes its degradation upon MPF inactivation in mitotic extracts of *Xenopus laevis* embryos. *Cell Cycle.* 5:1687–1698.

Cuschieri, L., T. Nguyen, and J. Vogel. 2007. Control at the cell center: the role of spindle poles in cytoskeletal organization and cell cycle regulation. *Cell Cycle.* 6:2788–2794.

D'Angiolella, V., C. Mari, D. Nocera, L. Rametti, and D. Grieco. 2003. The spindle checkpoint requires cyclin-dependent kinase activity. *Genes Dev.* 17:2520–2525. doi:10.1101/gad.267603

De Souza, C.P., and S.A. Osmani. 2007. Mitosis, not just open or closed. *Eukaryot. Cell.* 6:1521–1527. doi:10.1128/EC.00178-07

De Souza, C.P.C., A.H. Osmani, S.B. Hashmi, and S.A. Osmani. 2004. Partial nuclear pore complex disassembly during closed mitosis in *Aspergillus nidulans*. *Curr. Biol.* 14:1973–1984. doi:10.1016/j.cub.2004.10.050

De Souza, C.P., S.B. Hashmi, T. Nayak, B. Oakley, and S.A. Osmani. 2009. Mlp1 acts as a mitotic scaffold to spatially regulate spindle assembly checkpoint proteins in *Aspergillus nidulans*. *Mol. Biol. Cell.* 20:2146–2159. doi:10.1091/mbc.E08-08-0878

Fernández-Abalos, J.M., H. Fox, C. Pitt, B. Wells, and J.H. Doonan. 1998. Plant-adapted green fluorescent protein is a versatile vital reporter for gene expression, protein localization and mitosis in the filamentous fungus, *Aspergillus nidulans*. *Mol. Microbiol.* 27:121–130. doi:10.1046/j.1365-2958.1998.00664.x

Glotzer, M. 1995. Cell cycle. The only way out of mitosis. *Curr. Biol.* 5:970–972. doi:10.1016/S0960-9822(95)00190-4

Glotzer, M., A.W. Murray, and M.W. Kirschner. 1991. Cyclin is degraded by the ubiquitin pathway. *Nature.* 349:132–138. doi:10.1038/349132a0

Hagting, A., C. Karlsson, P. Clute, M. Jackman, and J. Pines. 1998. MPF localization is controlled by nuclear export. *EMBO J.* 17:4127–4138. doi:10.1093/emboj/17.14.4127

Horio, T., and B.R. Oakley. 2005. The role of microtubules in rapid hyphal tip growth of *Aspergillus nidulans*. *Mol. Biol. Cell.* 16:918–926. doi:10.1091/mbc.E04-09-0798

Hoyt, M.A., L. Totis, and B.T. Roberts. 1991. *S. cerevisiae* genes required for cell cycle arrest in response to loss of microtubule function. *Cell.* 66:507–517. doi:10.1016/0092-8674(81)90014-3

Huang, J., and J.W. Raff. 1999. The disappearance of cyclin B at the end of mitosis is regulated spatially in *Drosophila* cells. *EMBO J.* 18:2184–2195. doi:10.1093/emboj/18.8.2184

Jaspersen, S.L., J.F. Charles, R.L. Tinker-Kulberg, and D.O. Morgan. 1998. A late mitotic regulatory network controlling cyclin destruction in *Saccharomyces cerevisiae*. *Mol. Biol. Cell.* 9:2803–2817.

Job, D., O. Valiron, and B. Oakley. 2003. Microtubule nucleation. *Curr. Opin. Cell Biol.* 15:111–117. doi:10.1016/S0955-0674(02)00003-0

Jung, M.K., N. Prigozhina, C.E. Oakley, E. Nogales, and B.R. Oakley. 2001. Alanine-scanning mutagenesis of *Aspergillus* gamma-tubulin yields diverse and novel phenotypes. *Mol. Biol. Cell.* 12:2119–2136.

Kornbluth, S., C. Smythe, and J.W. Newport. 1992. In vitro cell cycle arrest induced by using artificial DNA templates. *Mol. Cell. Biol.* 12:3216–3223.

Lange, B.M.H. 2002. Integration of the centrosome in cell cycle control, stress response and signal transduction pathways. *Curr. Opin. Cell Biol.* 14:35–43. doi:10.1016/S0955-0674(01)00291-5

Lee, S.B., and J.W. Taylor. 1990. Isolation of DNA from fungal mycelia and single spores. *In* PCR Protocols: A Guide to Methods and Applications. M.A. Innis, D.H. Gelfand, J.J. Sninsky, and T.J. White, editors. Academic Press, San Diego. pp 282–287.

Li, R., and A.W. Murray. 1991. Feedback control of mitosis in budding yeast. *Cell.* 66:519–531. doi:10.1016/0092-8674(81)90015-5

Mikule, K., B. Delaval, P. Kaldis, A. Jurcyzk, P. Hergert, and S. Doxsey. 2007. Loss of centrosome integrity induces p38-p53-p21-dependent G1-S arrest. *Nat. Cell Biol.* 9:160–170. doi:10.1038/ncb1529

Mirabito, P.M., and N.R. Morris. 1993. BIMA, a TPR-containing protein required for mitosis, localizes to the spindle pole body in *Aspergillus nidulans*. *J. Cell Biol.* 120:959–968. doi:10.1083/jcb.120.4.959

Morris, N.R. 1975. Mitotic mutants of *Aspergillus nidulans*. *Genet. Res.* 26:237–254. doi:10.1017/S0016672300016049

Müller, H., M.L. Fogeron, V. Lehmann, H. Lehrach, and B.M.H. Lange. 2006. A centrosome-independent role for gamma-TuRC proteins in the spindle assembly checkpoint. *Science.* 314:654–657. doi:10.1126/science.1132834

Murray, A.W., M.J. Solomon, and M.W. Kirschner. 1989. The role of cyclin synthesis and degradation in the control of maturation promoting factor activity. *Nature.* 339:280–286. doi:10.1038/339280a0

Musacchio, A., and E.D. Salmon. 2007. The spindle-assembly checkpoint in space and time. *Nat. Rev. Mol. Cell Biol.* 8:379–393. doi:10.1038/nrm2163

Nayak, T., E. Szewczyk, C.E. Oakley, A. Osmani, L. Ukil, S.L. Murray, M.J. Hynes, S.A. Osmani, and B.R. Oakley. 2006. A versatile and efficient gene-targeting system for *Aspergillus nidulans*. *Genetics.* 172:1557–1566. doi:10.1534/genetics.105.052563

Nigg, E.A. 1995. Cyclin-dependent protein kinases: key regulators of the eukaryotic cell cycle. *Bioessays.* 17:471–480. doi:10.1002/bies.950170603

Nishiyama, A., K. Tachibana, Y. Igarashi, H. Yasuda, N. Tanahashi, K. Tanaka, K. Ohsumi, and T. Kishimoto. 2000. A nonproteolytic function of the proteasome is required for the dissociation of Cdc2 and cyclin B at the end of M phase. *Genes Dev.* 14:2344–2357. doi:10.1101/gad.823200

Nurse, P. 1990. Universal control mechanism regulating onset of M-phase. *Nature.* 344:503–508. doi:10.1038/344503a0

O'Connell, M.J., A.H. Osmani, N.R. Morris, and S.A. Osmani. 1992. An extra copy of *nim*E^{cyclinB} elevates pre-MPF levels and partially suppresses mutation of *nim*T^{cdc25} in *Aspergillus nidulans*. *EMBO J.* 11:2139–2149.

O'Donnell, K.L., A.H. Osmani, S.A. Osmani, and N.R. Morris. 1991. *bimA* encodes a member of the tetratricopeptide repeat family of proteins and is required for the completion of mitosis in *Aspergillus nidulans*. *J. Cell Sci.* 99:711–719.

Oakley, B.R. 2000. gamma-Tubulin. *Curr. Top. Dev. Biol.* 49:27–54. doi:10.1016/S0070-2153(99)49003-9

Oakley, C.E., C.F. Weil, P.L. Kretz, and B.R. Oakley. 1987. Cloning of the *ribo*B locus of *Aspergillus nidulans*. *Gene.* 53:293–298. doi:10.1016/0378-1119(87)90019-9

Osmani, A.H., N. van Peij, M. Mischke, M.J. O'Connell, and S.A. Osmani. 1994. A single p34^{cdc2} protein kinase (encoded by *nimX*^{cdc2}) is required at G_1 and G_2 in *Aspergillus nidulans*. *J. Cell Sci.* 107:1519–1528.

Osmani, A.H., J. Davies, H.L. Liu, A. Nile, and S.A. Osmani. 2006. Systematic deletion and mitotic localization of the nuclear pore complex proteins of *Aspergillus nidulans*. *Mol. Biol. Cell.* 17:4946–4961. doi:10.1091/mbc.E06-07-0657

Pines, J., and C.L. Rieder. 2001. Re-staging mitosis: a contemporary view of mitotic progression. *Nat. Cell Biol.* 3:E3–E6. doi:10.1038/35050676

Prigozhina, N.L., C.E. Oakley, A.M. Lewis, T. Nayak, S.A. Osmani, and B.R. Oakley. 2004. gamma-tubulin plays an essential role in the coordination of mitotic events. *Mol. Biol. Cell.* 15:1374–1386. doi:10.1091/mbc.E03-06-0405.

Shaner, N.C., R.E. Campbell, P.A. Steinbach, B.N. Giepmans, A.E. Palmer, and R.Y. Tsien. 2004. Improved monomeric red, orange and yellow fluorescent proteins derived from *Discosoma* sp. red fluorescent protein. *Nat. Biotechnol.* 22:1567–1572. doi:10.1038/nbt1037

Sluder, G. 2005. Two-way traffic: centrosomes and the cell cycle. *Nat. Rev. Mol. Cell Biol.* 6:743–748. doi:10.1038/nrm1712

Son, S., and S.A. Osmani. 2009. Analysis of all protein phosphatase genes in *Aspergillus nidulans* identifies a new mitotic regulator, fcp1. *Eukaryot. Cell.* 8:573–585. doi:10.1128/EC.00346-08

Stegmeier, F., and A. Amon. 2004. Closing mitosis: the functions of the Cdc14 phosphatase and its regulation. *Annu. Rev. Genet.* 38:203–232. doi:10.1146/annurev.genet.38.072902.093051

Suelmann, R., N. Sievers, and R. Fischer. 1997. Nuclear traffic in fungal hyphae: *in vivo* study of nuclear migration and positioning in *Aspergillus nidulans*. *Mol. Microbiol.* 25:757–769. doi:10.1046/j.1365-2958.1997.5131873.x

Szewczyk, E., T. Nayak, C.E. Oakley, H. Edgerton, Y. Xiong, N. Taheri-Talesh, S.A. Osmani, B.R. Oakley, and B. Oakley. 2006. Fusion PCR and gene targeting in *Aspergillus nidulans*. *Nat. Protoc.* 1:3111–3120. doi:10.1038/nprot.2006.405

Todd, R.B., J.A. Fraser, K.H. Wong, M.A. Davis, and M.J. Hynes. 2005. Nuclear accumulation of the GATA factor AreA in response to complete nitrogen starvation by regulation of nuclear export. *Eukaryot. Cell.* 4:1646–1653. doi:10.1128/EC.4.10.1646-1653.2005

Toews, M.W., J. Warmbold, S. Konzack, P. Rischitor, D. Veith, K. Vienken, C. Vinuesa, H. Wei, and R. Fischer. 2004. Establishment of mRFP1 as a fluorescent marker in *Aspergillus nidulans* and construction of expression vectors for high-throughput protein tagging using recombination in vitro (GATEWAY). *Curr. Genet.* 45:383–389. doi:10.1007/s00294-004-0495-7

van Leuken, R., L. Clijsters, and R. Wolthuis. 2008. To cell cycle, swing the APC/C. *Biochim. Biophys. Acta.* 1786:49–59.

Vardy, L., and T. Toda. 2000. The fission yeast gamma-tubulin complex is required in G(1) phase and is a component of the spindle assembly checkpoint. *EMBO J.* 19:6098–6111. doi:10.1093/emboj/19.22.6098

Vishniac, W., and M. Santer. 1957. The *thiobacilli*. *Bacteriol. Rev.* 21:195–213.

Visintin, R., K. Craig, E.S. Hwang, S. Prinz, M. Tyers, and A. Amon. 1998. The phosphatase Cdc14 triggers mitotic exit by reversal of Cdk-dependent phosphorylation. *Mol. Cell.* 2:709–718. doi:10.1016/S1097-2765(00)80286-5

Wakefield, J.G., J.Y. Huang, and J.W. Raff. 2000. Centrosomes have a role in regulating the destruction of cyclin B in early *Drosophila* embryos. *Curr. Biol.* 10:1367–1370. doi:10.1016/S0960-9822(00)00776-4

Waring, R.B., G.S. May, and N.R. Morris. 1989. Characterization of an inducible expression system in *Aspergillus nidulans* using *alcA* and tubulin-coding genes. *Gene.* 79:119–130. doi:10.1016/0378-1119(89)90097-8

Weidner, G., C. d'Enfert, A. Koch, P.C. Mol, and A.A. Brakhage. 1998. Development of a homologous transformation system for the human pathogenic fungus *Aspergillus fumigatus* based on the *pyrG* gene encoding orotidine 5′-monophosphate decarboxylase. *Curr. Genet.* 33:378–385. doi:10.1007/s002940050350

Wiese, C., and Y. Zheng. 1999. Gamma-tubulin complexes and their interaction with microtubule-organizing centers. *Curr. Opin. Struct. Biol.* 9:250–259. doi:10.1016/S0959-440X(99)80035-9

Wong, O.K., and G. Fang. 2007. Cdk1 phosphorylation of BubR1 controls spindle checkpoint arrest and Plk1-mediated formation of the 3F3/2 epitope. *J. Cell Biol.* 179:611–617. doi:10.1083/jcb.200708044

Wu, L., S.A. Osmani, and P.M. Mirabito. 1998. A role for NIMA in the nuclear localization of cyclin B in *Aspergillus nidulans*. *J. Cell Biol.* 141:1575–1587. doi:10.1083/jcb.141.7.1575

Yang, J., E.S. Bardes, J.D. Moore, J. Brennan, M.A. Powers, and S. Kornbluth. 1998. Control of cyclin B1 localization through regulated binding of the nuclear export factor CRM1. *Genes Dev.* 12:2131–2143. doi:10.1101/gad.12.14.2131

Yang, L., L. Ukil, A. Osmani, F. Nahm, J. Davies, C.P. De Souza, X. Dou, A. Perez-Balaguer, and S.A. Osmani. 2004. Rapid production of gene replacement constructs and generation of a green fluorescent protein-tagged centromeric marker in *Aspergillus nidulans*. *Eukaryot. Cell.* 3:1359–1362. doi:10.1128/EC.3.5.1359-1362.2004

Ye, X.S., R.R. Fincher, A. Tang, A.H. Osmani, and S.A. Osmani. 1998. Regulation of the anaphase-promoting complex/cyclosome by *bimA*^{APC3} and proteolysis of NIMA. *Mol. Biol. Cell.* 9:3019–3030.